PCCP

PAPER

Cite this: *Phys. Chem. Chem. Phys.*, 2017, **19**, 2044

Is energy transfer limiting multiphotochromism? answers from *ab initio* quantifications†

Arnaud Fihey,*[ab] Roberto Russo,[c] Lorenzo Cupellini,[c] Denis Jacquemin*[bd] and Benedetta Mennucci*[c]

Received 1st November 2016,
Accepted 15th December 2016

DOI: 10.1039/c6cp07458h

www.rsc.org/pccp

Dithienylethenes (DTEs) can be assembled to form supramolecular multiphotochromic systems that are highly functional molecular architectures of potential interest for building complex optoelectronic devices. Yet even simple DTE dimers relying on an organic linker may suffer from a partial photoactivity, *i.e.*, only one of the two switches does isomerise. Experimentally, this limited photochromism has been attributed to an excited state energy transfer (EET) between the two DTEs of the multimer; this EET taking place instead of the desired photoinduced cyclisation of the DTE. However, no clear evidences of this phenomenon have been provided so far. In this work we propose the first rationalisation of this potential parasite photoinduced event using a computational approach based on Time-Dependent Density Functional Theory (TD-DFT) for the calculation of the electronic coupling in DTE dimers. Besides quantifying EET in several systems, we dissect the role of through-bond and through-space mechanisms on this process and clarify their dependence on both the nature and length of the bridge separating the two photochromes. The theoretical data obtained in this framework are in full agreement with the experimental outcomes and pave the way toward a molecular design of coupled, yet fully functionals, DTE-based multiswitches.

1 Introduction

Photochromism in organic molecules paves the way towards remotely controlled nano-sized devices.[1–3] During the course of development of these light-responsive materials, and amongst the numerous series of efficient organic photochromes, some families of switches have been clearly more popular, namely, azobenzene and dithienylethene (DTE) derivatives. Their photophysical and photochemical properties have been thoroughly investigated both experimentally[4,5] and theoretically.[6–8] Several successful applications of the hallmark switching mechanism of these compounds have also been reported.[9–11] DTE-based photochromic systems usually exhibit robust switching properties as they benefit from the thermal irreversibility and the high repeatability[12] of their isomerisation process that connects a generally non-coloured open form and a more conjugated closed form that absorbs in the visible (see Fig. 1). Those two isomers can be used to store a bit of information (0 = open; 1 = closed), as well as to modulate the conductance between two contacts (“on” = conducting, closed; “off” = isolating, open).[13] Likewise, they have also been used to induce light-controlled movement in flexible polymers.[14] Beyond the binary functionality of isolated photoactive units, a wide variety of systems combining two or more organic switches have been recently designed[15–19] and the multiphotochromic DTE assemblies stand as the most popular subgroup of this ensemble. If the combination of n photochromic entities can in principle result in 2^n distinct states, the design of fully-functional objects has however encountered numerous issues.[20,21]

When building such supramolecular switches, the main parameter influencing the photoactivity of the resulting compound has been clearly proven to be the nature of the organic bridge linking the photochromic units.[20] Depending on the spatial separation and the amount of electronic communication brought by this linker, distinct scenarios are indeed observed. For multimers in which the DTEs are weakly coupled, *e.g.*, are separated by a long or saturated bridge, the constituting photochromes preserve their intrinsic optical properties. If all DTEs are identical this leads to the same photoactivity as in the isolated switches, but for an increase of the intensity of the optical response proportional to the number of photochromes. For instance, it has been observed in a star-shaped molecule

[a] *Institut des Sciences Chimiques de Rennes, UMR 6226 CNRS, Université de Rennes1, 263 Av. du Général Leclerc, 35042, Cedex Rennes, France. E-mail: Arnaud.Fihey@univ-rennes1.fr*
[b] *CEISAM, UMR CNRS 6230, Université de Nantes, 2, Rue de la Houssinière, BP 92208, 44322 Nantes, Cedex 3, France. E-mail: Denis.Jacquemin@univ-nantes.fr*
[c] *Dipartimento di Chimica e Chimica Industriale, Universitá di Pisa, via G. Moruzzi 13, 56124 Pisa, Italy. E-mail: benedetta.mennucci@unipi.it*
[d] *Institut Universitaire de France, 1 rue Descartes, 75231 Paris Cedex 5, France*

† Electronic supplementary information (ESI) available: Cartesian coordinates and orbital representations. See DOI: 10.1039/c6cp07458h

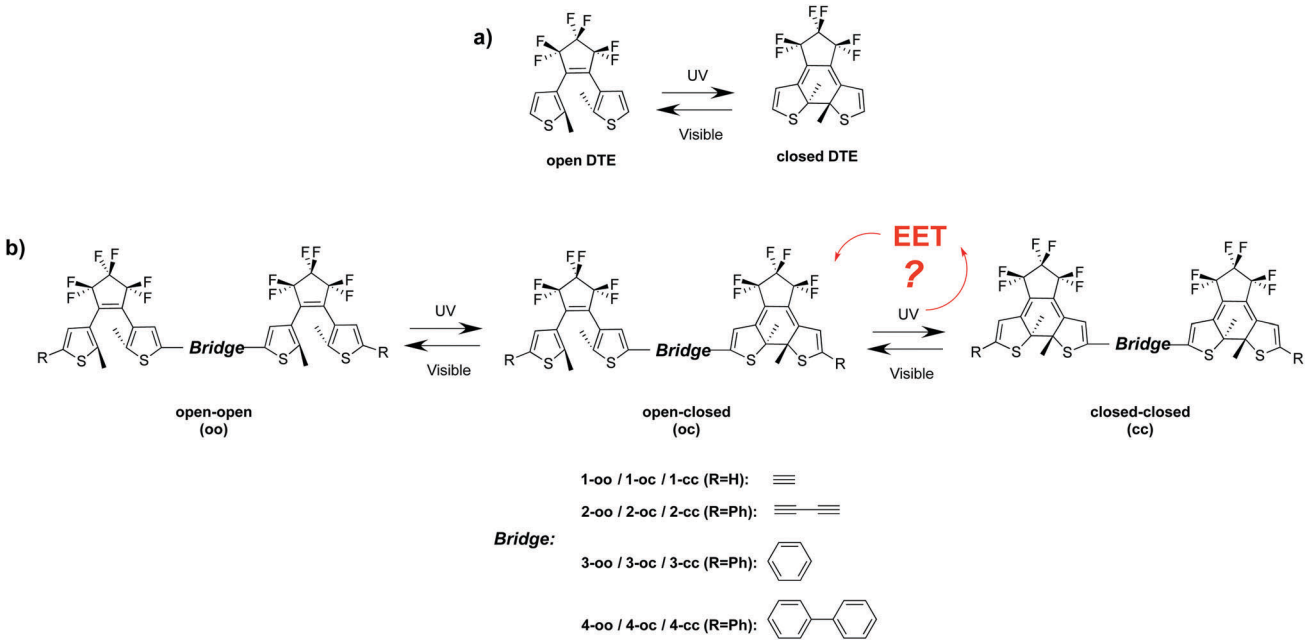

Fig. 1 (a) Isomerisation process in a typical DTE and (b) in the dimers investigated herein.

presenting six DTEs that the full isomerisation can be achieved under irradiation with UV light.[19] In that case, no intermediate presenting only a fraction of closed DTE was detected using absorption spectroscopy. The same holds in DTE dyads using a linker limiting the electronic communication: all DTE isomerisation occur simultaneously on the experimental timescale.[22–25] It is clear that the most effective way to design a multiphotochromic system presenting emerging functionalities (beyond the simple addition of the responses of the components) is to use a bridge allowing for significant electronic or steric interactions between the different constituting photoactive units.[26–31] A few successful examples of this strategy can be found,[29,30] in which, for instance, a phenyl linker separating two identical DTEs allows for the isolation of an intermediate open–closed isomer before the formation of the fully closed isomer. Nevertheless, in numerous cases,[26,31] the photocyclisation of the DTEs remains beyond reach, regardless of the irradiation time: partial photochromism is observed. Approximately half of the experimental DTE dimers designed so far are subject to this limitation,[20] that remains to be fully understood. Most theoretical works dealing with DTE have been dedicated to the predictions of the effects of the chemical substitution on the UV-Visible spectra,[32–35] and only a few provided clues regarding mutiphotochromism.[21,36–38] These latter investigations typically relied on a static Time-Dependent Density Functional Theory (TD-DFT) analysis of the nature of the electronic transitions. However, the prediction and quantification of the possible excited-state energy transfer (EET) competing with the photochromic reaction were not performed to date, though such process has been pointed out in the experimental works to account for the observed partial photochromism.[39] More specifically, in a DTE dimer presenting one closed and one open DTE, an energy transfer is expected to take place from the excited-state of the open DTE acting as a donor (D) to the closed DTE acting as an acceptor (A). In a Förster type energy transfer, this mechanism is justified by the electronic coupling between D and A, and by the overlap of the emission and absorption densities of states of D and A, respectively. The excited-state of the open DTE responsible for the isomerisation to the closed form is then "deactivated" by this EET, and multiphotochromism is not achieved.

How EET takes place in conjugated organic chromophores and how it is impacted by the nature of the bridge separating the donor and the acceptor moieties has been a subject of numerous experimental and theoretical studies.[40–42] It is clear that the model selected to quantify EET has to be carefully chosen to accurately describe the key underlying physical phenomena. For instance, typical cases in which the Förster model needs to be improved are: (i) the failure of the point-dipolar approximation at short-distances where "heterogeneity" is needed;[43] (ii) a distance dependent screening of the surrounding medium;[44,45] and (iii) bridge-mediated contribution to the D/A coupling, often referred to as "superexchange" effects.[42] For instance in π-extended supramolecules with intramolecular energy transfer,[46] such effects have to be accounted for to reach an accurate reproduction of the experimental photophysics.[47] In this context, theoretical schemes using a quantum chemical descriptions are adequate tools to model EET. If excited-state quantum dynamics can ultimately describe the migration of an excitation within the D/A system along time,[48] some of us also showed that a less cumbersome "static" TD-DFT model allows bypassing the above-listed limitations of standard models thanks to the calculation of the electronic coupling between the excited-states. Such TD-DFT approach considers the interaction between the transition densities of the D and A moieties,[49–51] and allows quantifying the EET between these two moieties in the supramolecule. For instance considering

BODIPY derivatives or porphyrin dyads, it has been shown that the theoretical EET rate could be used to quantitatively explain the observed photophysical outcomes.[52–54]

The goal of the present study is to provide the first theoretical quantification of the potential energy transfer in photochromic multimers by applying such TD-DFT based model for determining the electronic coupling. In particular we investigate four different DTE dimers presenting different organic bridges between the two photochromic units (see Fig. 1). Compounds **1**[26] and **2**[55] are typical of partially active dimers in which the doubly closed isomer is not formed experimentally even after prolonged UV irradiation. In contrast, dimer **3**[30] is fully active and the three possible isomers can be formed and isolated. Finally, **4** has, to our knowledge, not been synthesised yet but is designed as a less communicating dimer where the coupling between the two DTEs is expected to be lower, therefore avoiding the pitfall of partial photochromism. For these multiphotochromic compounds, we first briefly investigate the vertical absorption properties based on the analysis of the electronic transitions obtained at the TD-DFT level to obtain first insights into their photochromic behaviour. In a second step we focus on describing and quantifying the EET between the two DTEs. More precisely we detail the influence of the frontier chosen to define the donor and the acceptor fragments on the obtained coupling. In order to achieve a complete understanding of the role of the bridge, we analyse the electronic coupling in terms of its ''through-space'' and ''through-bond'' contributions. This work is, to the best of our knowledge, the first theoretical effort to quantify the potential EET mechanism as the cause of the experimental limited photochromic behaviour in coupled multiphotochromic derivatives.

2 Methods and computational details

2.1 Methods

We only briefly summarise the theoretical approach below. Indeed, the TD-DFT based model used here to compute the EET has been extensively described elsewhere,[49–51] and we redirect the interested readers to these earlier works for details. In DTEs, the photochemical process leads to a large reorganisation of the structure, therefore the coupling between the electronic excitation and the nuclear motions is much bigger than the interaction between the electronic states. In such weak coupling limit, the energy transfer rate can be described with the Fermi Golden Rule,

$$k_{\mathrm{EET}} = \frac{2\pi}{\hbar}|V|^2 J, \tag{1}$$

where V is the electronic coupling between the excitation of the donor (D) and acceptor (A) fragments, and J is the spectral overlap, namely the overlap integral between the absorption band of the acceptor with the emission band of the donor. In the linear response (LR) approach, the electronic couplings, V, are calculated beyond the point-dipolar approximation as the interaction between the transition densities (ρ^{tr}) of D and A.[56] For an isolated D/A pair, this coupling reads

$$\begin{aligned} V_{\mathrm{DA}} &= \int \mathrm{d}\mathbf{r} \int \mathrm{d}\mathbf{r}' \rho_{\mathrm{D}}^{\mathrm{tr}*}(r) \frac{1}{|r-r'|} \rho_{\mathrm{A}}^{\mathrm{tr}}(r') \\ &\quad + \int \mathrm{d}\mathbf{r} \int \mathrm{d}\mathbf{r}' \rho_{\mathrm{D}}^{\mathrm{tr}*}(r) g_{\mathrm{xc}}(r,r') \rho_{\mathrm{A}}^{\mathrm{tr}}(r') \\ &\quad - \omega_0 \int \mathrm{d}\mathbf{r} \rho_{\mathrm{D}}^{\mathrm{tr}}(r) \rho_{\mathrm{A}}^{\mathrm{tr}}(r). \end{aligned} \tag{2}$$

The first term in eqn (2) is the Coulomb interaction between transition densities, which dominates the coupling for bright transitions. The second term is an exchange–correlation interaction, where g_{xc} is the exchange–correlation kernel of the DFT functional used. The Coulomb-exchange–correlation coupling is finally corrected by an overlap contribution (ω_0 is the average resonance transition energy of the dimer). In the presence of the solvent, V_{DA} contains an additional solvent-mediated term, given by the interaction between the transition density of the donor and the solvent response to the transition of the acceptor.[56] Within the Polarisable Continuum Model (PCM) framework this additional term is defined in terms of a set of induced charges (q) on the surface of the molecular cavity embedding the chromophore, namely:

$$V_{\mathrm{solv}} = \sum_k \left(\int \mathrm{d}r \rho_{\mathrm{D}}^{\mathrm{tr}}(r) \frac{1}{|r-s_k|} \right) q\left(s_k; \varepsilon_\infty, \rho_{\mathrm{A}}^{\mathrm{tr}}\right), \tag{3}$$

where q is the solvent response induced by $\rho_{\mathrm{A}}^{\mathrm{tr}}$, and mediated by the optical dielectric permittivity $\varepsilon_\infty = n^2$. s_k labels the position of the k^{th} tesserae building the PCM cavity.

In addition to screening the Coulomb interaction, the solvent affects the coupling through its impact on the transition properties of the donor and the acceptor. This change can be seen as an ''implicit effect'', as opposed to the explicit effect described by eqn (3).

2.2 Computational details

The ground-state geometries of the DTE dimers were optimised at the DFT level using the PBE0[57] global hybrid functional associated with the 6-31+G(d) atomic basis set. Vibrational frequencies calculations were systematically conducted at the same level of theory, to ensure that the obtained structures are true energy minima. TD-DFT was used to determine the transition properties. Here the TD-DFT calculations relied on a range-separated hybrid functional, CAM-B3LYP,[58] and the 6-311G(d) atomic basis set, as such approach has been proven to yield accurate optical properties for DTE monomers and multimers.[37] Solvent effects were included in the PCM framework to match the experimental UV-Visible measurement conditions (*n*-hexane), using the non-equilibrium linear response formalism, for both the geometry optimisation and the TD-DFT steps (computation of the vertical transitions and the electronic coupling). All calculations were conducted with a locally modified version of the Gaussian09 software.[59]

3 Results and discussion

3.1 UV-Visible absorption of the dimers

The analysis of the topologies of the virtual molecular orbitals involved in the vertical electronic transitions can provide first hints regarding the feasibility of the ring closing in DTE monomers and multimers.[20,36,37,60] More precisely, one can evaluate the possibility to form (or not) a closed DTE by considering the presence (or the absence) in the open DTE spectrum, of an energetically-accessible electronic transition promoting the electron towards a virtual molecular orbital presenting a bonding contribution between the two carbon atoms forming the new CC bond during the cyclisation process. Such transition can be referred to as a "photochromic transition" and the associated virtual orbital as a "photochromic orbital".[21] In such very simplified framework, the observed efficiency of the first photocyclisation (**oo** → **oc**) in the considered dimers can be understood by examining the first electronic transitions in the doubly open form. The lowest-energy transition always mainly corresponds to a HOMO → LUMO excitation peaking at *ca.* 300 nm. For instance, this intense (f = 1.15) transition is found at 333 nm in **1-oo**, and the LUMO is clearly a photochromic orbital (see Fig. 2). Irradiating in the UV is therefore predicted to yield the formation of the mixed open–closed isomer **1-oc**, consistently with experiment.[26] The same conclusion holds for the three other fully open dimers.

For the second photocyclisation (**oc** → **cc**) of main interest for this work, the analysis is typically less straightforward.[36] Table 1 lists the electronic transitions populating a photochromic orbital in the open–closed isomers. For all derivatives, the first intense low-lying transition appears in the visible domain and involves, as expected, the LUMO located on the most π-conjugated fragment, namely, the closed DTE moiety (see Fig. 2). The first virtual orbital located on the open DTE and possessing photochromic features is the LUMO+1 for **1-oc**, **3-oc** and **4-oc**, and the LUMO+2 for **2-oc** (sketched in Fig. 2). These orbitals are clearly localised on the open DTE in **1-oc** and **3-oc**, while they are partly delocalised along the bridge in **4-oc**. Ultimately for **2-oc** the delocalisation takes place along the full system including the closed DTE. In all four open–closed systems, TD-DFT predicts that only two electronic transitions in the UV domain significantly populate these orbitals (see Table 1). In **1-oc**, these two transitions are found to be moderately intense (f of 0.07 and 0.06) but lead to a large population of the photochromic orbital (>50%). In contrast, in **2-oc**, these two transitions are more intense (f of 0.22 and 0.12) but involve a smaller share of the LUMO+1. **3-oc** and **4-oc** behave similarly, with two energetically close photochromic transitions (289 nm and 280 nm in **3-oc**, 279 nm and 278 nm in **4-oc**), the former being very intense but involving only moderately the LUMO+1 (14%); the opposite trend is found for the latter transition. In short, the photochromic orbital of the open–closed isomers is poorly (strongly) populated by the intense (weak) transitions and none of the investigated open–closed dimers can be predicted to yield the fully closed form in a totally unambiguous fashion. Nevertheless, differences between the derivatives can be underlined. The most striking is the energetic proximity of the two photochromic transitions in **3-oc** and **4-oc**, while they are well separated in **1-oc** and **2-oc**. We recall that both **1** and **2** have been shown to exhibit partial photochromism only, whereas the fully closed isomer could be reached in **3**, which cannot be obviously deduced from the results of Table 1. Therefore, in the following, we show that quantifying EET is a more efficient approach for predicting the photochromic behaviour of the **oc** systems.

Table 1 Photochromic transitions in the open–closed dimers. The photochromic orbital (PO) is given along with the wavelength (nm) and the oscillator strength (f) of the transition involving the PO in an ratio given as a percentage in the rightmost column. Only transitions above 250 nm and with a f exceeding 0.05 are listed

Compound	PO	Wavelength (f)	Population (%)
1-oc	LUMO+1	294 (0.07)	51
		268 (0.06)	85
2-oc	LUMO+2	327 (0.22)	15
		294 (0.12)	55
3-oc	LUMO+1	289 (0.70)	14
		280 (0.13)	77
4-oc	LUMO+1	279 (0.89)	14
		278 (0.12)	71

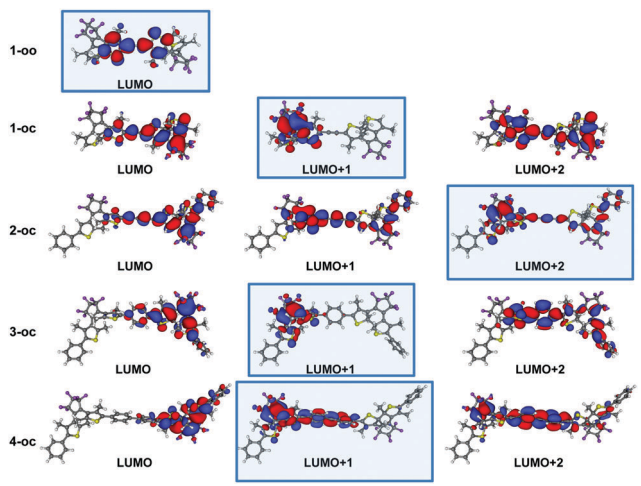

Fig. 2 Representation of the key virtual molecular orbitals in **1-oo** and in the open–closed forms isomers of **1–4** (isocontour: 0.02 au). Photochromic orbitals are indicated with a blue background.

3.2 Electronic coupling

Choice of a cutting model. To model an energy transfer process, the dimer has first to be decomposed into two fragments, D (open DTE) and A (closed DTE). As those two moieties are covalently linked through an organic linker, bonds separating the DTEs and the bridge, or within the bridge itself, have to be cut and saturated by a capping hydrogen atom to create spatially well-defined fragments. If the choice of a specific border is straightforward when a saturated chemical group breaks the π-conjugation between D and A,[53] this is not the case here. Indeed, one has to separate D and A from a significantly coupled entity where the bridge is not totally

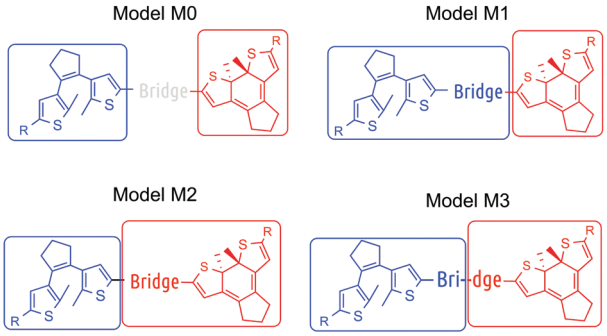

Fig. 3 The four different cut models employed to evaluate the coupling between DTEs.

innocent and may bear electronic density for the states of interest, as illustrated in Fig. 2. As no *a priori* choice prevails, we investigate different cutting scenarios as illustrated in Fig. 3. "Model 1", noted M1, assigns the bridge to the donor moiety, that is, the open DTE, whereas M2 connects the linker to the closed DTE (acceptor). When possible, *i.e.*, for dimers **2** and **4**, we also considered M3 where the bridge is cut in its midpoint. Eventually, a model where the bridge is not taken into-account (M0) was applied to describe the through-space component of the coupling. The consideration of several types of fragments counterbalances the fact that the fragments are defined within an electronically communicating dyad. Indeed, the variations of the couplings resulting from the different cutting possibilities provide insights into the role of the bridge in the EET process. This is why the coupling values returned by the different cutting models are first discussed in the following for each dimer by considering the topology of the D and A electronic states, before rationalizing the experimental facts by quantifying the variations of the coupling between the four open–closed dyads.

The labels and transition densities of the different fragments are displayed in Fig. 4.[61] To determine the electronic coupling, one needs to identify the excited-states taking part in the potential energy migration mechanism. For the donor moieties, the excited-state should involve one of the "photochromic orbitals" as described above. In all open DTE fragments, the state of interest is unambiguously the lowest excited-state, and corresponds to an intense HOMO → LUMO transition, typical of DTE in their open form;[20] the activation of this state by irradiation at *ca.* 300 nm is expected to trigger the photocyclisation if no quenching takes place. The only exception is fragment D_4 in which the third excited-state was chosen as the photochromic donor state, as the two lower states are localised on the conjugated double ethynyl bridge instead of the DTE core. The relevant state on the acceptor fragment (closed DTE) was selected by, on the one hand, checking that the state is bright (non-negligible oscillator strength), and, on the other hand, that its energy is close but lower than the energy of the donor state. This acceptor state is the third excited-state in all closed fragments but in A_4, where the fourth excited-state better matches the energy of the D fragment.

Fragments' optical properties. The transition densities of the open and closed DTE fragments are represented in Fig. 4.

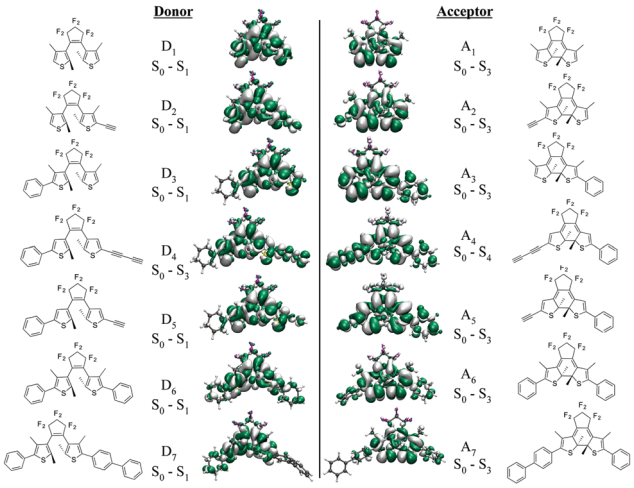

Fig. 4 Representation of the transition densities for the fragments in their open and closed forms (isocontour: 0.0009 au for green areas, −0.0009 au for white areas).

The associated excitation energies and oscillator strengths are listed in Table 2. Considering fragments not incorporating the bridge in the backbone, and taking D_1 and A_1 as non-substituted references, we note that the presence of an external phenyl ring, as in dimers **2**, **3** and **4**, to obtain fragments D_3 and A_3 yields only a very small perturbation of the $S_0 \rightarrow S_1$ (open D) and $S_0 \rightarrow S_3$ (closed A) transition densities. This is consistent with the twist between the thienyl and phenyl moieties that limits direct π-conjugation. Likewise, the same occurs when a phenyl-based bridge is taken into account. Indeed, the transition densities of fragments D_6 and D_7 and their closed counterparts A_6 and A_7 do not show significant transition densities on the linker. The open fragments D_2, D_4 and D_5 and closed fragments A_2, A_4 and A_5, which all contain an ethynyl moiety, exhibit excited-states with roughly the same topology as in the D_1/A_1 fragments, though the delocalisation along the bridge is clearly more pronounced than in the phenyl-based fragments. Indeed the open D_2 and closed A_4 fragments, encompassing one and two triple-bond terminations

Table 2 Electronic transition energies (in eV) and oscillator strengths of the different fragments

Dimer	Model	D	$E(f)$	A	$E(f)$
1-oc	M0	D_1	4.480 (0.11)	A_1	4.310 (0.02)
	M1	D_2	4.390 (0.09)	A_1	4.310 (0.02)
	M2	D_1	4.480 (0.11)	A_2	4.262 (0.06)
2-oc	M0	D_3	4.328 (0.14)	A_3	4.302 (0.16)
	M1	D_4	4.239 (0.19)	A_3	4.302 (0.16)
	M2	D_3	4.328 (0.14)	A_4	3.958 (0.22)
	M3	D_5	4.239 (0.18)	A_5	4.163 (0.34)
3-oc	M0	D_3	4.475 (0.10)	A_3	4.332 (0.04)
	M1	D_6	4.385 (0.13)	A_3	4.332 (0.04)
	M2	D_3	4.475 (0.10)	A_6	4.233 (0.08)
4-oc	M0	D_3	4.498 (0.10)	A_3	4.363 (0.03)
	M1	D_7	4.459 (0.08)	A_3	4.363 (0.03)
	M2	D_3	4.498 (0.10)	A_7	4.326 (0.01)
	M3	D_6	4.463 (0.08)	A_6	4.329 (0.02)

respectively, are the fragments for which the amplitudes of the transition density on the bridge are the largest. Following eqn (2), those differences in the transition density of the fragments composing the dyad are expected to greatly impact the calculated coupling values, discussed below.

Total electronic coupling. The electronic couplings have been computed on the ground-state equilibrium geometries, as one can assume that the coupling values do not change significantly upon geometrical reorganisation. In addition, the EET should be faster than the relaxation if it competes with the cyclisation. We also underline that the efficiency of the EET is discussed in the following by focussing on the electronic coupling, V_{DA}, because the amount of available spectroscopic information is too limited to allow an accurate calculation of the spectral overlap, J, and hence the direct access to the energy transfer rates, k_{EET}, defined in eqn (1). A first approximation of k_{EET} is nevertheless given using an arbitrary J value, assumed to be constant in the dimer series.

Table 3 lists both the total electronic coupling V_{DA} and its different contributions as defined in eqn (2) and (3): the V_{Coul} (Coulombic), V_{xc} (exchange) and V_{solv} (screening by the solvent) contributions. When examining the V_{DA} values, two distinct behaviours clearly appear. On the one hand, **1-oc** and **2-oc**, and, on the other hand, **3-oc** and **4-oc**. For the former dimers, the couplings are strongly dependent on the selected cutting model. For instance, going from the M0 model to either the M1 and M2 models results in a large increase of the coupling values. Indeed, they are found to go from 4.3 cm^{-1} and 6.6 cm^{-1} with M0 to 25.3 cm^{-1} and 48.0 cm^{-1} with M2, for **1-oc** and **2-oc**, respectively. In the absence of the bridge (M0), the only interaction between the two fragments is the Coulomb coupling between the DTE-localised transitions. When the bridge is included in the donor part, the transition density partially delocalises on the bridge, which increases the Coulomb interaction. We refer to this effect as a ''SuperCoulomb'' effect. The 48.0 cm^{-1} V_{DA} value for **2-oc** is the largest coupling reported in Table 3, and the same compound described with M1 also returns a very high coupling of 32.2 cm^{-1}. Interestingly, in the M3 model that splits the bridge on both the D and A sides, a lower V_{DA} is obtained: a fraction of the interaction between the two moieties is lost in this model and the coupling is undershot. This indicates that an accurate picture of the effects of the linker can be achieved only if this bridge is not fragmented. Overall, dimer **2-oc** undergoes the largest coupling, undoubtedly because: (i) the excited-states of interest in both the D and the A moieties present large oscillator strengths compared to the other compounds; and (ii) the transition density is well delocalised on the bridge linking the two DTEs (see also the orbitals in Fig. 2). Notably, in **1-oc**, the value of V_{DA} calculated with the M1 model (2.0 cm^{-1}) is much smaller than with M2 (25.3 cm^{-1}), and even lower than with M0 (4.3 cm^{-1}). In order to understand this result, we considered separately the different terms in eqn (2). In model M0, the Coulomb contribution to the coupling is largely dominant, albeit screened by the explicit solvent term of eqn (3). The Coulomb and explicit contributions (respectively, 5.9 and −1.5 cm^{-1}) remain unchanged in model M1, but the exchange contribution, of opposite sign, is responsible for the decrease of the coupling value. In contrast, model M2 presents a much larger Coulomb contribution to the coupling, which can be explained by the large increase of the oscillator strength of the acceptor state when the bridge is considered (see Table 2). In chemical terms, the transition density of the acceptor is largely delocalised on the ethynyl bridge, close to the donor transition density, and largely enhances the interaction. Notably, the oscillator strength of the donor is slightly reduced when the bridge is considered, yielding a negative contribution to the Coulomb interaction with the acceptor. The effect of the bridge is critical in these two dimers and induces large variations of the V_{DA}. This is in line with a previous joint theoretical/experimental study on a perylene monoimide (D)/terrylene diimide (A) system bridged with a π-conjugated linker. In that case, only the consideration of the bridge within the appropriate moiety allowed reaching an agreement with the spectroscopic measurements, therefore avoiding an underestimation of the coupling.[62] For the highly communicating dimers treated here, the difference in the coupling values is not to be attributed to a failure of the D/A interaction due to the transition density model but to the necessity of selecting a suited fragment-cutting model to grasp the correct amount of through-bridge ''superexchange'' interaction (see Introduction). Here, the large couplings between the two DTEs in both **1-oc** and **2-oc** for the M2 model, where the bridge is considered along with the acceptor, account for significant EET and hence the deactivation of the excited-state of the open side in agreement with the experimental observation of a partial photochromic activity.

For dimers **3-oc** and **4-oc** possessing a phenyl-based bridge, the coupling remains rather low (smaller than 10 cm^{-1}), regardless of the fragment model selected. In **3-oc**, a moderate increase of the coupling is observed when using M1 or M2 model instead of M0, while in **4-oc**, the different models all lead very small coupling values. This illustrates the negligible influence of the phenyl–phenyl linker on the excited-state properties

Table 3 Theoretical total electronic coupling (V_{DA}) and the different contributions (V_{Coul}, V_{xc} and V_{solv}) for different D/A pairs of the open–closed dimers, considering different separation models. All couplings are in cm^{-1}

Dimer	Model	Fragments	V_{DA}	V_{Coul}	V_{xc}	V_{solv}
1-oc	M0	D_1/A_1	4.3	5.9	−0.1	−1.5
	M1	D_2/A_1	2.0	5.3	−1.9	−1.4
	M2	D_1/A_2	25.3	30	2.7	−7.5
2-oc	M0	D_3/A_3	6.6	10.0	0.0	−3.3
	M1	D_4/A_3	33.2	102.6	−23.7	−31.1
	M2	D_3/A_4	48.0	38.4	1.8	−7.1
	M3	D_5/A_5	18.4	39.5	−7.7	−13.5
3-oc	M0	D_3/A_3	2.7	3.4	0.0	−0.7
	M1	D_6/A_3	8.6	13.6	−4.1	−1.0
	M2	D_3/A_6	9.4	16.8	−3.2	−4.3
4-oc	M0	D_3/A_3	2.0	2.9	0.0	−0.9
	M1	D_7/A_3	0.5	0.7	0.0	−0.1
	M2	D_3/A_7	2.1	3.1	−0.1	−0.8
	M3	D_6/A_6	1.2	1.8	0.0	−0.6

of the constitutive DTEs, as the presence, the absence or the separation of this bridge into two identical parts, always deliver V_{DA} between 0 and 2 cm^{-1}: no efficient EET can take place and the photochromism of the two units is preserved. The fundamental reasons explaining this outcome can be traced back to the transition densities given in Fig. 4: no significant transition density lies on the linker. Therefore, treating the linker at the quantum-mechanical level does not bring significant changes as almost no orbital overlap is present. In addition, the large distance separating the two DTEs in the **4-oc** dimer logically lowers the Coulomb interaction.

In summary, within the series of compounds investigated, **1-oc** and **2-oc** present the highest V_{DA} values, and more importantly, this coupling strongly increases when the bridge is taken into account: the linker is clearly influencing the electronic communication between the excited-states of the two photochromes. The energy migration after the electronic excitation of the open DTE towards the closest fragment is consequently sped up by the presence of ethynyl-based linkers, and ultimately the EET becomes competitive with the photocyclisation of DTE, in agreement with the partial photochromism observed for these two systems.[26,55] In contrast, for the two other dimers V_{DA} is almost independent of the cutting model and the computed total coupling remains systematically low. This is in the line with the reported total photochromism in **3**:[30] EET in **3-oc** is not efficient enough to quench cyclisation. According to our analysis, the same should holds for the newly designed dimer **4**. As noted in the beginning of this section, by setting arbitrarily the J overlap in eqn (1) to 1 eV, a typical value for conjugated organic compounds,[53,63] we compute EET rates of *ca.* 10^{11}–10^{12} for **1-oc** and **2-oc**. This yields a transfer time in the 3–10 ps range, which is indeed faster than the typical photocylisation time of DTE (*ca.* 10 ps).[64] For **3-oc** and **4-oc**, EET rates of *ca.* 10^{7}–10^{10} are determined, indicating an energy transfer speed in the 80–2000 ps domain, slower than the cyclisation time. To the best of our knowledge, these values stand as the first quantitative estimates of the EET rates in DTE multimers, and importantly, they are consistent with the experimental outcomes. Beyond the framework of molecular switches, we recall that numerous experimental,[65] theoretical,[66] or joint experimental and theoretical studies[67] compared the changes in the excitonic couplings in non-photochromic D/A dyes pair upon variation of the structure of the bridge. These works were mainly focussed on structurally identical linkers of different lengths, that is, oligomers. Direct comparisons between phenyl and ethynyl bridges connecting the same D/A pair is, to our knowledge, unprecedented.

3.3 Through-space *versus* through-bond contributions

To clarify the role of the linker in the different systems, we have divided the total coupling into two contributions only. They are clearly related to the role played by the linker. The first one, namely the Through-Space (TS) component, consists in the Coulomb interaction between the transition densities of the isolated donor and acceptor. The second, namely the Through-Bond (TB) contribution, is constituted of the interaction

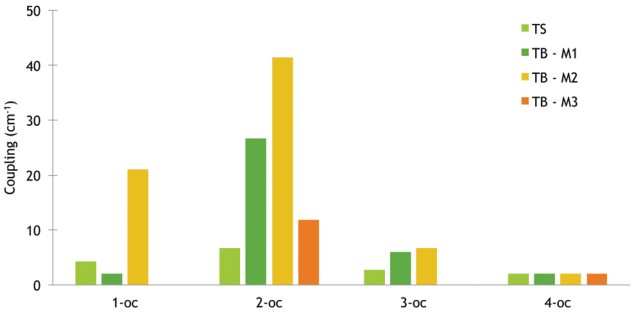

Fig. 5 Representation of the absolute TB and TS contributions in the total coupling for the different open–closed dimers, and for different models.

mediated by the bridge, *i.e.*, the electronic exchange interaction, as well as the longer-range interactions, *i.e.*, the Super-Coulomb mechanism. The former describes the Dexter mechanism, where the interaction decays exponentially with distance, whereas the latter is related to the participation of the bridge in the transition density. The TS contribution can be determined with the M0 model: when the bridge is absent the interactions are purely Coulombic as the DTEs are too distant to allow overlap between their orbitals. In the other models, M1, M2 and M3, in which the linker is described at the QM level, we define the TB contribution as the part of the coupling due to the bridge:

$$\begin{aligned} V_{\mathrm{Tot}} &= V_{\mathrm{TS}} + V_{\mathrm{TB}}, \\ V_{\mathrm{TS}} &= V_{\mathrm{M0}}. \end{aligned} \tag{4}$$

Fig. 5 gives the magnitude of these TS and TB contributions for the four dimers. In **1-oc** and **2-oc**, which have been highlighted as possessing strong couplings, that increase when the bridge is taken into account, the TB contribution clearly appears to be dominating. It represents more than 80% of the total coupling in the M2 model for **1-oc**, and in both the M1 and M2 models for **2-oc**. In **2-oc** the TB coupling, that is the preponderant contribution, ranges from 11.8 cm^{-1} to 41.4 cm^{-1}, and remains larger than its TS counterpart, irrespective of the selected model. In **3-oc**, the bridge plays a less important role in the excited-state communication and the TB contributions is much smaller than in **2-oc**, while in **4-oc** there is no significant communication between the two DTE moieties. Indeed, both TS and TB are trifling (smaller than 2 cm^{-1}) when a bi-phenyl bridge is used.

The difference of photoactivity between the partially active ethynyl-based dimers and the fully active phenyl-based dimer is clearly related to the through-bond contribution that is the decisive term determining the magnitude of the total coupling. Indeed, in the full series, the TS contribution always remains quite small (6.6 cm^{-1} at most).

4 Conclusions

The present work stands as the first to provide quantitative estimates for the coupling between the DTEs in

multiphotochromic compounds. Previously, the prediction of the reactivity of these complex entities mainly relied on the analysis of the virtual orbitals populated by the absorption of light,[21] but such approach can provide qualitative insights only. Similarly, the more refined curve crossing model developed recently by some of us,[68] delivers a chemically-intuitive picture but does not allow to estimate the relative speeds of the competing excited-state processes and is, at this stage, limited to the weak coupling limit. Here, considering four DTE dimers including two that showed partial photocyclisation experimentally, we modeled the excited-state energy transfer between the two photochromes, as this process was previously evoked as the quenching mechanism responsible for the loss of reactivity of the open DTE in the hybrid open–closed dimer. To this end, we applied a TD-DFT approach considering the open DTE as the donor and the closed DTE as the acceptor, and used several fragmentation schemes to gain insights into the communication between the excited states of the two covalently-linked DTEs. Including the bridge in the fragments induces large increase of the couplings for the ethynyl systems but small changes for the phenyl dyads. The decomposition of the electronic coupling demonstrated that the through-space (Coulomb) component is rather independent of the nature of the linker, whereas the through-bond (orbital overlap and SuperCoulomb) component is sensitive to the chemical nature of the bridge and therefore guides the final outcome. The estimated EET speeds show that energy transfer is faster than the typical cyclisation in the partially active dyads, but slower in the fully active dimers. The magnitudes of the electronic couplings calculated in the considered series are therefore in perfect agreement with the experimental facts, and we trust that this kind of theoretical analysis is, to date, the most relevant for predicting and rationalising the photoactivity of multiphotochromic compounds, even when strong couplings take place. This approach opens a new way to design multiswitches using *ab initio* tools. In this vein, more complex architectures will be next studied, some incorporating several kinds of photochromes,[69] some more than two DTEs,[19,70] and some more complex bridges.[71]

Acknowledgements

A. F. and D. J. are indebted to Dr B. Lasorne for fruitful discussions. A. F. acknowledges the European Research Council (ERC, Marches – 278845) for supporting his post-doctoral grant in Nantes. D. J. acknowledges the ERC and the *Région des Pays de la Loire* for financial support in the framework of a Starting Grant (Marches – 278845) and the LUMOMAT project, respectively. B. M. acknowledges the European Research Council (ERC) for financial support in the framework of the Starting Grant (EnLight – 277755). All authors acknowledge the support of the CNRS in the framework of the SodasPret PICS project. This research used resources of CCIPL (*Centre de Calcul Intensif des Pays de Loire*), and a local Troy cluster.

References

1 M. Irie, Y. Yokoyama and T. Seki, *New Frontiers in Photochromism*, Springer, Japan, 2013.
2 H. Dürr and H. Bouas-Laurent, *Photochromism: Molecules and Systems*, Elsevier Science, 1st edn, 2003.
3 W. R. B. Ben and L. Feringa, *Molecular Switches*, Wiley-VCH Verlag GmbH & Co. KGaA, 2nd edn, 2011.
4 M. Irie, T. Fukaminato, K. Matsuda and S. Kobatake, *Chem. Rev.*, 2014, **114**, 12174–12277.
5 Z. F. Liu, K. Hashimoto and A. Fujishima, *Nature*, 1990, **347**, 658–660.
6 P. D. Patel and A. E. Masunov, *J. Phys. Chem. C*, 2011, **115**, 10292–10297.
7 Y. Asano, A. Murakami, T. Kobayashi, A. Goldberg, D. Guillaumont, S. Yabushita, M. Irie and S. Nakamura, *J. Am. Chem. Soc.*, 2004, **126**, 12112–12120.
8 R. J. Maurer and K. Reuter, *Chem. Phys.*, 2011, **135**, 224303.
9 S. Kawata and Y. Kawata, *Chem. Rev.*, 2000, **100**, 1777–1788.
10 D. Gust, J. Andreasson, U. Pischel, T. A. Moore and A. L. Moore, *Chem. Commun.*, 2012, **48**, 1947–1957.
11 G. Copley, T. A. Moore, A. L. Moore and D. Gust, *Adv. Mater.*, 2013, **25**, 456–461.
12 M. Herder, B. M. Schmidt, L. Grubert, M. Pätzel, J. Schwarz and S. Hecht, *J. Am. Chem. Soc.*, 2015, **137**, 2738–2747.
13 F. Meng, Y.-M. Hervault, L. Norel, K. Costuas, C. Van Dyck, V. Geskin, J. Cornil, H. H. Hng, S. Rigaut and X. Chen, *Chem. Sci.*, 2012, **3**, 3113–3118.
14 J.-i. Mamiya, A. Kuriyama, N. Yokota, M. Yamada and T. Ikeda, *Chem. – Eur. J.*, 2015, **21**, 3174–3177.
15 S. Kobatake, S. Kuma and M. Irie, *Bull. Chem. Soc. Jpn.*, 2004, **77**, 945–951.
16 S. Saita, T. Yamaguchi, T. Kawai and M. Irie, *ChemPhysChem*, 2005, **6**, 2300–2306.
17 B. Li, H.-M. Wen, J.-Y. Wang, L.-X. Shi and Z.-N. Chen, *Inorg. Chem.*, 2013, **52**, 12511–12520.
18 B. Li, J.-Y. Wang, H.-M. Wen, L.-X. Shi and Z.-N. Chen, *J. Am. Chem. Soc.*, 2012, **134**, 16059–16067.
19 J. Areephong, H. Logtenberg, W. R. Browne and B. L. Feringa, *Org. Lett.*, 2010, **12**, 2132–2135.
20 A. Fihey, A. Perrier, W. R. Browne and D. Jacquemin, *Chem. Soc. Rev.*, 2015, **44**, 3719–3759.
21 A. Perrier, F. Maurel and D. Jacquemin, *Acc. Chem. Res.*, 2012, **45**, 1173–1182.
22 E. A. Shilova, A. Heyndrickx and O. Siri, *J. Org. Chem.*, 2010, **75**, 1855–1861.
23 W. Tan, X. Li, J. Zhang and H. Tian, *Dyes Pigm.*, 2011, **89**, 260–265.
24 H. J. Kim, J. H. Jang, H. Choi, T. Lee, J. Ko, M. Yoon and H.-J. Kim, *Inorg. Chem.*, 2008, **47**, 2411–2415.
25 S. Kuehn, S. Friede, M. Zastrow, K. Schiebler, K. Rueck-Braun and T. Elsaesser, *Chem. Phys. Lett.*, 2013, **555**, 206–211.
26 T. Kaieda, S. Kobatake, H. Miyasaka, M. Murakami, N. Iwai, Y. Nagata, A. Itaya and M. Irie, *J. Am. Chem. Soc.*, 2002, **124**, 2015–2024.
27 K. Higashiguchi, K. Matsuda, N. Tanifuji and M. Irie, *J. Am. Chem. Soc.*, 2005, **127**, 8922–8923.

28 H.-h. Liu and Y. Chen, *J. Mater. Chem.*, 2011, **21**, 1246–1249.
29 K. Matsuda and M. Irie, *J. Am. Chem. Soc.*, 2001, **123**, 9896–9897.
30 S. Kobatake and M. Irie, *Tetrahedron*, 2003, **59**, 8359–8364.
31 H. Wang, W. Xu and D. Zhu, *Tetrahedron*, 2012, **68**, 8719–8723.
32 P. D. Patel and A. E. Masunov, *J. Phys. Chem. A*, 2009, **113**, 8409–8414.
33 I. Mikhailov and A. Masunov, in *Computational Science – ICCS 2009*, ed. G. Allen, J. Nabrzyski, E. Seidel, G. van Albada, J. Dongarra and P. Sloot, Springer Berlin Heidelberg, 2009, vol. 5545, pp. 169–178.
34 A. D. Laurent, X. Assfeld, D. Jacquemin, J.-M. André and E. A. Perpète, *Mol. Simul.*, 2010, **36**, 74–78.
35 A. Perrier, F. Maurel and J. Aubard, *J. Photochem. Photobiol. A: Chem.*, 2007, **189**, 167–176.
36 D. Jacquemin, E. A. Perpète, F. Maurel and A. Perrier, *J. Phys. Chem. C*, 2010, **114**, 9489–9497.
37 A. Fihey and D. Jacquemin, *Chem. Sci.*, 2015, **6**, 3495–3504.
38 A. Fihey, A. Perrier and F. Maurel, *J. Photochem. Photobiol. A: Chem.*, 2012, **247**, 30–41.
39 T. Kawai, T. Sasaki and M. Irie, *Chem. Commun.*, 2001, 711–712.
40 B. Albinsson, M. P. Eng, K. Pettersson and M. U. Winters, *Phys. Chem. Chem. Phys.*, 2007, **9**, 5847–5864.
41 B. Albinsson and J. Mårtensson, *J. Photochem. Photobiol., C*, 2008, **9**, 138–155.
42 B. Albinsson and J. Martensson, *Phys. Chem. Chem. Phys.*, 2010, **12**, 7338–7351.
43 G. D. Scholes, *Annu. Rev. Phys. Chem.*, 2003, **54**, 57–87.
44 C. Curutchet, G. D. Scholes, B. Mennucci and R. Cammi, *J. Phys. Chem. B*, 2007, **111**, 13253–13265.
45 G. D. Scholes, C. Curutchet, B. Mennucci, R. Cammi and J. Tomasi, *J. Phys. Chem. B*, 2007, **111**, 6978–6982.
46 R. Métivier, F. Nolde, K. Müllen and T. Basché, *Phys. Rev. Lett.*, 2007, **98**, 047802.
47 B. Fückel, A. Köhn, M. E. Harding, G. Diezemann, G. Hinze, T. Basché and J. Gauss, *J. Chem. Phys.*, 2008, **128**, 074505.
48 J. F. Galindo, E. Atas, A. Altan, D. G. Kuroda, S. Fernandez-Alberti, S. Tretiak, A. E. Roitberg and V. D. Kleiman, *J. Am. Chem. Soc.*, 2015, **137**, 11637–11644.
49 C. Curutchet, A. Muñoz-Losa, S. Monti, J. Kongsted, G. D. Scholes and B. Mennucci, *J. Chem. Theory Comput.*, 2009, **5**, 1838–1848.
50 S. Caprasecca, C. Curutchet and B. Mennucci, *J. Chem. Theory Comput.*, 2012, **8**, 4462–4473.
51 B. Mennucci and C. Curutchet, *Phys. Chem. Chem. Phys.*, 2011, **13**, 11538–11550.
52 S. Caprasecca, C. Curutchet and B. Mennucci, *Photochem. Photobiol. Sci.*, 2011, **10**, 1602–1609.
53 M. Di Donato, A. Iagatti, A. Lapini, P. Foggi, S. Cicchi, L. Lascialfari, S. Fedeli, S. Caprasecca and B. Mennucci, *J. Phys. Chem. C*, 2014, **118**, 23476–23486.
54 S. Caprasecca, C. Curutchet and B. Mennucci, *J. Phys. Chem. C*, 2013, **117**, 12423–12431.
55 B. Li, Y.-H. Wu, H.-M. Wen, L.-X. Shi and Z.-N. Chen, *Inorg. Chem.*, 2012, **51**, 1933–1942.
56 M. F. Iozzi, B. Mennucci, J. Tomasi and R. Cammi, *J. Chem. Phys.*, 2004, **120**, 7029–7040.
57 C. Adamo and V. Barone, *J. Chem. Phys.*, 1999, **110**, 6158–6170.
58 T. Yanai, D. P. Tew and N. C. Handy, *Chem. Phys. Lett.*, 2004, **393**, 51–57.
59 M. J. Frisch, G. W. Trucks, H. B. Schlegel, G. E. Scuseria, M. A. Robb, J. R. Cheeseman, G. Scalmani, V. Barone, B. Mennucci, G. A. Petersson, H. Nakatsuji, M. Caricato, X. Li, H. P. Hratchian, A. F. Izmaylov, J. Bloino, G. Zheng, J. L. Sonnenberg, M. Hada, M. Ehara, K. Toyota, R. Fukuda, J. Hasegawa, M. Ishida, T. Nakajima, Y. Honda, O. Kitao, H. Nakai, T. Vreven, J. A. Montgomery, Jr., J. E. Peralta, F. Ogliaro, M. Bearpark, J. J. Heyd, E. Brothers, K. N. Kudin, V. N. Staroverov, R. Kobayashi, J. Normand, K. Raghavachari, A. Rendell, J. C. Burant, S. S. Iyengar, J. Tomasi, M. Cossi, N. Rega, J. M. Millam, M. Klene, J. E. Knox, J. B. Cross, V. Bakken, C. Adamo, J. Jaramillo, R. Gomperts, R. E. Stratmann, O. Yazyev, A. J. Austin, R. Cammi, C. Pomelli, J. W. Ochterski, R. L. Martin, K. Morokuma, V. G. Zakrzewski, G. A. Voth, P. Salvador, J. J. Dannenberg, S. Dapprich, A. D. Daniels, Ö. Farkas, J. B. Foresman, J. V. Ortiz, J. Cioslowski and D. J. Fox, *Gaussian 09 Revision D.01*, Gaussian Inc., Wallingford CT, 2009.
60 A. D. Laurent, J. M. André, E. A. Perpète and D. Jacquemin, *J. Photochem. Photobiol. A: Chem.*, 2007, **192**, 211–219.
61 We note that some fragments, *e.g.*, D_3 and A_4, exist with (in dimer **3**) and without (in dimer **2**) methyl group at the β position of the thiophene rings. In Fig. 4, only one of the two possibilities is given for clarity purpose, as this methyl group has a very slight impact on the transition densities.
62 C. Curutchet, F. A. Feist, B. V. Averbeke, B. Mennucci, J. Jacob, K. Mullen, T. Basche and D. Beljonne, *Phys. Chem. Chem. Phys.*, 2010, **12**, 7378–7385.
63 O. Yushchenko, R. V. Hangarge, S. Mosquera-Vazquez, S. V. Boshale and E. Vauthey, *J. Phys. Chem. B*, 2015, **119**, 7308–7320.
64 Y. Ishibashi, M. Fujiwara, T. Umesato, H. Saito, S. Kobatake, M. Irie and H. Miyasaka, *J. Phys. Chem. C*, 2011, **115**, 4265–4272.
65 M. Gilbert and B. Albinsson, *Chem. Soc. Rev.*, 2015, **44**, 845–862.
66 H.-C. Chen, Z.-Q. You and C.-P. Hsu, *J. Chem. Phys.*, 2008, **129**, 084708.
67 K. Pettersson, A. Kyrychenko, E. Ronnow, T. Ljungdahl, J. Martensson and B. Albinsson, *J. Phys. Chem. A*, 2006, **110**, 310–318.
68 B. Lasorne, A. Fihey, D. Mendive-Tapia and D. Jacquemin, *Chem. Sci.*, 2015, **6**, 5695–5702.
69 S. Bellotto, R. Reuter, C. Heinis and H. A. Wegner, *J. Org. Chem.*, 2011, **76**, 9826–9834.
70 Q. Luo, S. Cheng and H. Tian, *Tetrahedron Lett.*, 2004, **45**, 7737–7740.
71 J. Areephong, J. H. Hurenkamp, M. T. W. Milder, A. Meetsma, J. L. Herek, W. R. Browne and B. L. Feringa, *Org. Lett.*, 2009, **11**, 721–724.